Science Arts & Métiers (SAM)

is an open access repository that collects the work of Arts et Métiers Institute of Technology researchers and makes it freely available over the web where possible.

This is an author-deposited version published in: https://sam.ensam.eu
Handle ID: .http://hdl.handle.net/10985/9675

To cite this version :

Yang XIA, Maxence BIGERELLE, Salima BOUVIER, Alain IOST, Pierre-Emmanuel MAZERAN - Quantitative approach to determine the mechanical properties by nanoindentation test: Application on sandblasted materials - Tribology International - Vol. 82, p.297-304 - 2015

Any correspondence concerning this service should be sent to the repository Administrator : scienceouverte@ensam.eu

Arts et Métiers Institute of Technology

Quantitative approach to determine the mechanical properties by nanoindentation test: Application on sandblasted materials

Y. Xia [a], M. Bigerelle [b,*], S. Bouvier [a], A. Iost [c], P.-E. Mazeran [a]

[a] Laboratoire Roberval de Mécanique, Université de Technologie de Compiègne, 60205 Compiègne Cedex, France
[b] Matériaux, surfaces et mise en forme, TEMPO, LAMIH, Université de Valenciennes, 59313 Valenciennes, France
[c] Laboratoire MSMP, Arts et Métiers ParisTech, ENSAM, CS 50008, 59046 Lille Cedex, France

A B S T R A C T

A novel method is developed to improve the accuracy in determining the mechanical properties from nanoindentation curves. The key point of this method is the simultaneous statistical treatment of several loading curves to correct the zero point error and identify the material properties considering size effects. The method is applied to four sandblasted aluminum-based specimens with different surface roughness. A linear relationship is obtained between the standard deviation of the initial contact error and the roughness which highlights the effect of the surface roughness on the reproducibility of the indentation curves. Moreover, the smaller standard deviation of the hardness given by the method confirms the importance of considering the initial contact error for an accurate determination of the material properties.

Keywords:
Nanoindentation
Roughness
Sandblasting
Mechanical properties

1. Introduction

Mechanical properties play a crucial role in contact mechanics and should be determined accurately to predict the ability of a material to resist a plastic deformation, contact fatigue, and wear etc. Nanoindentation technique is largely used to determine mechanical properties near the surface [1]. However, in the specific case of rough surfaces, the low reproducibility of the load–depth curves due to a bad determination of the initial contact leads to an inaccurate estimation of the material properties (*e.g.* hardness) [2]. Experimentally, the initial contact corresponds to the smallest reachable applied load; or when the contact stiffness becomes higher to a value given by a user [3]. However, different problems may occur which affect the initial contact error, *e.g.* the geometry of the indenter tip, the instrument system errors (false detection), the surface preparation and the roughness [4]. In nanoindentation, the size of the imprint is too small to be measured accurately with optical microscopy. Therefore, the load–depth curve and the geometry of the indenter are used to determine the contact area and consequently the material hardness. In case of rough surface, as indicated previously, the determination of the initial contact depth becomes difficult, since the first contact points can be located on a valley or on a peak of the surface leading to an error in the value of the indentation depth and consequently in the true contact area [5]. Some methods have been proposed to determine the initial contact point by redefining the zero position [6] or using the slope of the indentation curve [7]. However, these methods were mainly applied on spherical indenters. Other authors propose to use a large set of nanoindentation tests, to quantify from each test the material properties. They average the computed data in order to characterize the material.

In the present work, a quantitative statistical method is used to analyze a set of nanoindentation curves based on an innovative simultaneous shifting of the loading curves [8–11]. The method highlights the influence of the roughness on nanoindentation curve and leads to a more accurate determination of the mechanical properties. This method is applied to four sandblasted aluminum-based alloy 2017A specimens, which are abraded using different treatment parameters. The macro-hardness and the indentation size effect parameter are estimated. In addition, the surface roughness effect on the initial contact point detection is evidenced and effectively considered to obtain a more accurate value of the macro-hardness.

2. Experimental details

2.1. Specimen preparation

The four specimens investigated in this study were extracted from a bar of aluminum-based alloy 2017A. The chemical composition in wt%: Zn (0.25), Mg (0.4–1.0), Cu (3.5–4.5), Cr (0.1), Mn (0.4–1.0), Fe (0.7), Si (0.2–0.8), Zr+Ti (0.25), Al (base). The disks

* Corresponding author. Tel.: +33 6 16 29 76 04.
E-mail address: Maxence.Bigerelle@univ-valenciennes.fr (M. Bigerelle).

were 30 mm in diameter and 20 mm thickness. To ensure all the samples have the same mechanical and topographical initial state, a pre-polishing with 120, 320 and 1000 silicon carbide grit papers and a fine polishing with a 3 μm grain size diamond DP-Spray lubricant were performed successively. The specimens were then sandblasted using a jet of Al_2O_3 particles with a diameter of approximately 500 μm in a CSF 70V (ARENA, France) machine. The parameters of the sandblasting process for different specimens named S1–S4 are listed in Table 1.

2.2. Roughness measurement

The topography of the treated specimens was measured using a three-dimensional (3D) roughness tactile profilometer TENCOR™ P10. The vertical sensitivity of the profilometer is 10 nm and the horizontal sensitivity is 50 nm. A stylus with a tip radius of 2 μm has been used to probe the surface under a 5×10^{-5} N load. Two-dimensional (2D) high-resolution profiles have been recorded with a measurement length of 5 mm at a speed of 200 μm/s. Each profile is described by 25,000 points (0.2 μm between each point). For each specimen, 30 profiles are recorded.

2.3. Nanoindentation

Nanoindentation experiments were conducted on four sandblasted surfaces using a Nano Indenter XP (MTS System) equipped with a Berkovich tip indenter. The Continuous Stiffness Measurement (CSM) method was used; the harmonic oscillation depth and frequency were 2 nm and 45 Hz, respectively. For each specimen, 100 nanoindentations were made with a constant strain rate equal 0.05 s^{-1} until an indentation depth of 3000 nm is achieved. Fig. 1 displays the loading section of the nanoindentation curves obtained for the specimen S4. To avoid any statistical artifacts, only the parts of the curves whose load value are less than 0.8 times the maximum load are kept.

Table 1
Sandblasting parameters for four 2017A specimens. The angle is the included angle between the spray gun and specimen surface.

Specimen	Pressure (bar)	Distance (cm)	Angle (deg)
S1	1	15	90
S2	1	30	90
S3	0.5	30	90
S4	0.5	30	60

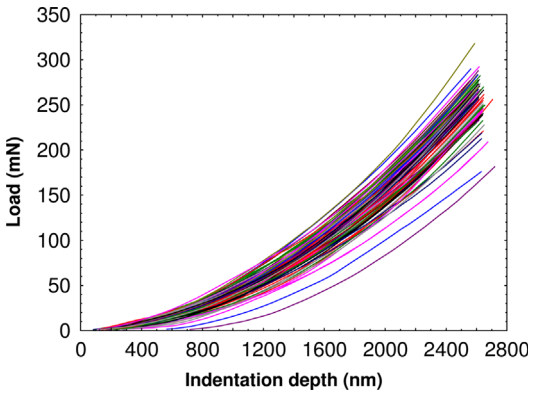

Fig. 1. Loading part of the load *versus* indentation depth curves for the sand blasted 2017A specimen S4.

3. Model and method

3.1. Multi-scale surface profile treatment

The evaluation length of surface profile has a critical effect on the roughness study [12]. Indeed, it was observed that different evaluation lengths will give different roughness parameters. The initial roughness profiles were experimentally measured for a given length. However, this length is so long comparing with the nanoindentation scale that is not suitable for nanoindentation study. A relevant evaluation length for the roughness calculation should be selected. Hence, the aim of the multi-scale surface profile treatment is to find the most suitable evaluation length of the surface roughness in nanoindentation study. In this treatment, the topographic profile was divided into equal parts whose length is the evaluation length. Then, a multi-scale composition of each original profile was carried out [13]. For one original topographic profile, the new profiles reset using different evaluation lengths are very different as shown in Fig. 2. Compared with the profile rectified using the shorter evaluation length (15 μm), the profile calculated using the longer evaluation length (521 μm) appears more wavy. The value of the quadratic roughness called R_q also depends on the evaluation length (Fig. 3). For each specimen, the quadratic roughness increases with an increasing evaluation length and approaches an asymptotic value. Comparing the four specimens, it can be observed that the surface roughness produced by different sandblasted parameters decreases from S1 to S4 whatever the evaluation lengths. It means that a higher jet pressure, shorter distance and bigger angle in sandblasting test produce rougher surface (higher R_q).

3.2. Load–depth curves treatment

Hardness is usually defined as

$$H = P/A_c, \tag{1}$$

where A_c is the contact area. With a Berkovich indenter, the contact area A_c can be expressed using the contact depth h_c:

$$A_c = \alpha h_c^2, \tag{2}$$

where α is depending on the geometry of the indenter, h_c is the real contact depth defined by Oliver and Pharr's method:

$$h_c = h - \varepsilon_{indenter}\frac{P}{S}, \tag{3}$$

where h is the measured displacement into the sample, S is the stiffness of contact and $\varepsilon_{indenter}$ is a geometrical constant equal to 0.75 for a Berkovich indenter. Thus, the previous equation becomes:

$$P = \alpha H h_c^2 \tag{4}$$

Then, we take into account the possibility of an Indentation Size effect (ISE, *i.e.* an increase in hardness with decreasing depth of penetration at small depths) through the use of Vingsbo's law [14] defined as

$$H = H_0 + \beta/h_c, \tag{5}$$

where H_0 is the macroscopic hardness and β is the ISE factor. It is worth noting that the linear relationship between the load and the penetration depth at the early stage of the indentation test gathers different phenomena known as the ISE. Such linear relationship yields to a proportionality between H and $1/h_c$, through a constant term, β, named ISE factor.

Thus, Eq. (4) is modified as follows:

$$P = \alpha(H_0 + \beta/h_c)h_c^2 = \alpha(H_0 h_c^2 + \beta h_c) \tag{6}$$

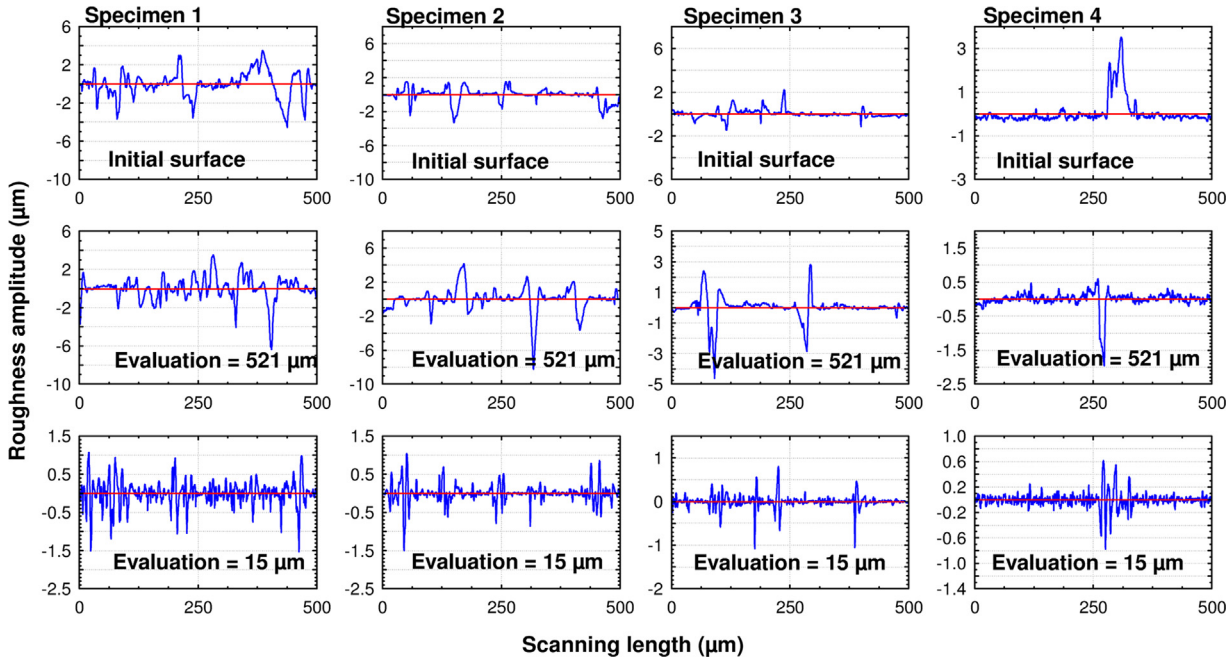

Fig. 2. Multi-scale profile reconstructions corresponding to different evaluation length.

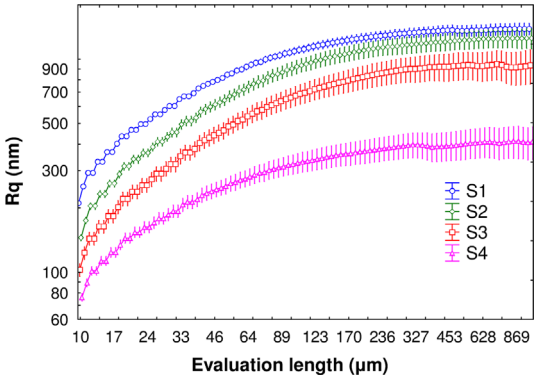

Fig. 3. Evolution of the Root Mean Square roughness (R_q) *versus* the evaluation lengths.

Eq. (6) is having a similar formula with the Bernhardt model [15], but different indentation depth is used in the equations as expressed by Eq. (7). The Bernhardt model uses the measured displacement into the sample, while the proposed model uses the real contact depth.

$$P = \alpha_1 h^2 + \alpha_2 h, \tag{7}$$

where h is the measured displacement into the sample, α_1 and α_2 are parameters related to the geometry of the indenter tip and the material properties.

In our method, all the experimental loading curves are firstly fitted by Eq. (6). A reference curve is arbitrarily selected from all the loading curves. Considering the original point of the reference curve is the reference initial contact point, the other loading curves could be written as follows:

$$P = \alpha[H_0(h_c + \Delta h_c)^2 + \beta(h_c + \Delta h_c)], \tag{8}$$

where Δh_c is the initial contact error, *i.e.* the distance between the experimental curves and the reference one in the indentation depth axis. Here, we suppose the macro-hardness and the ISE factor are constant for a specimen. A least-squares regression analysis is used to obtain the mechanical properties. It is a process of minimization to make the experimental curves best match the reference curve:

$$\min_{H_0, \Delta h_1 \ldots \Delta h_n, \beta} \sum_{i=1}^{n} \sum_{j=1}^{p_i} \{P_{i,j} - \alpha[H_0 h_{cj}^2 + (2H_0 \Delta h_{ci} + \beta) h_{cj} + H_0 \Delta h_{ci}^2 + \beta \Delta h_{ci}]\}^2, \tag{9}$$

where i is the ith loading curve and j refers to the jth couple point (P, h) of one loading curve.

The bootstrap is a statistical method of simple random sampling with replacement [16]. For getting the value of H_0 and β with their confidence intervals, a double bootstrap on the 100 original experimental loading curves of each specimen is performed. The first bootstrap is used to reduce the heterogeneity of material in gradient direction. It ensures that all the points in one curve are independent and identically distributed. The second bootstrap aims at reducing the variable of nanoindentation tests in different surface zone. It is also a good means to delete the error induced by the random choosing of the reference curve. For each bootstrap, the reference curve is chosen again. This process is repeated more than 1000 times in order to reduce the artificial factors.

3.3. Loading curves simulation

To investigate the effect of the initial contact point errors on the macro-hardness and ISE factor determination, a numerical simulation of load–depth curves has been performed for each specimen. The numerical curves are created according to Eq. (6), where the macro-hardness H_0 and ISE factor β are equal to the mean value identified by the proposed model based on the experimental data. The placement of numerical curves is only defined by the standard deviation of the initial contact error (σ_Δ). In the first part, the systemic origin of all the numerical curves is supposed at the zero of x-axis. Each numerical curve is placed along the x-axis according to the Gaussian distribution with different standard deviations. In the second part, we suppose that there is a gap between the systemic origin of all the numerical curves and the zero of the x-axis, note as Δ. Then each numerical curve is placed along the x-axis conforming to the Gaussian distribution with different standard deviation. The number of numerical curves is equal to the number of experimental curves for each specimen.

4. Results and discussion

4.1. Surface roughness and initial contact error correction

The experimental nanoindentation curves of the four sandblasted 2017A specimens with different roughness have been treated using the proposed method. Fig. 4 plots the loading curves of S4 after the shifting with the initial contact errors. Obviously, the shifted curves are closer than the original experimental curves shown in Fig. 1. It suggests that the error on the initial contact point detection could be reduced by the model.

The distribution of the initial contact error for each sandblasted 2017A specimen calculated based on the statistical method using a double Bootstrap has been shown in Fig. 5. It could be observed that the standard deviation of the initial contact error, which could be described as the width of red fitting line, decreases with the surface roughness from S1 to S4. For this reason, the investigation of relationship between the roughness and the standard deviation of initial contact error is valuable for quantifying the effect of surface roughness on nanoindentation data. As described in previous Section 3.1, the evaluation length is an important factor on the studying of surface roughness. Hence, the primary issue is to find the most appropriate evaluation length of roughness analysis in the nanoindentation study. Firstly, a multiplicity of calculations on surface roughness R_q has been done using different evaluation lengths for each specimen. Then the linear regressions between the calculated surface roughness R_q and the standard deviation of initial contact error $\sigma(\Delta h_c)$ have been studied to find the strongest correlation. Fig. 6 shows the plot of linear coefficient of determination (R^2) *versus* the different evaluation lengths. It is clear to see that there is a high correlation between the roughness R_q and the standard deviation of the initial contact error when the evaluation length is around 15 μm. It means the best evaluation length of roughness identification in this nanoindentation test is 15 μm, which is also in the size of the indentation print. In this scale, the indenter can be considered as a surface "probe". In other words, the initial contact error correction is just like shifting the indentation curves according to the amplitude of surface topography. Fig. 7 depicts the best linear relation between the standard deviation of initial contact error and the surface roughness R_q (standard deviation of the amplitude of surface topography) calculated with the evaluation length of 15 μm. It shows the effectiveness of the initial contact error correction. The proposed model allows predicting the mechanical properties based on nanoindentation test on sandblasted surface without link to the roughness itself.

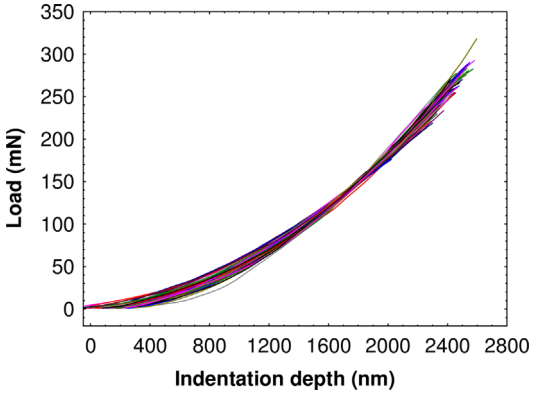

Fig. 4. Shifted load *versus* indentation depth curves for the sand blasted 2017A specimen S4.

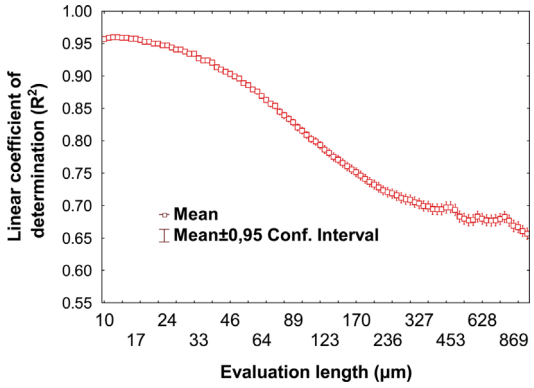

Fig. 6. Evolution of the linear correlation coefficient (R^2) *versus* different evaluation lengths.

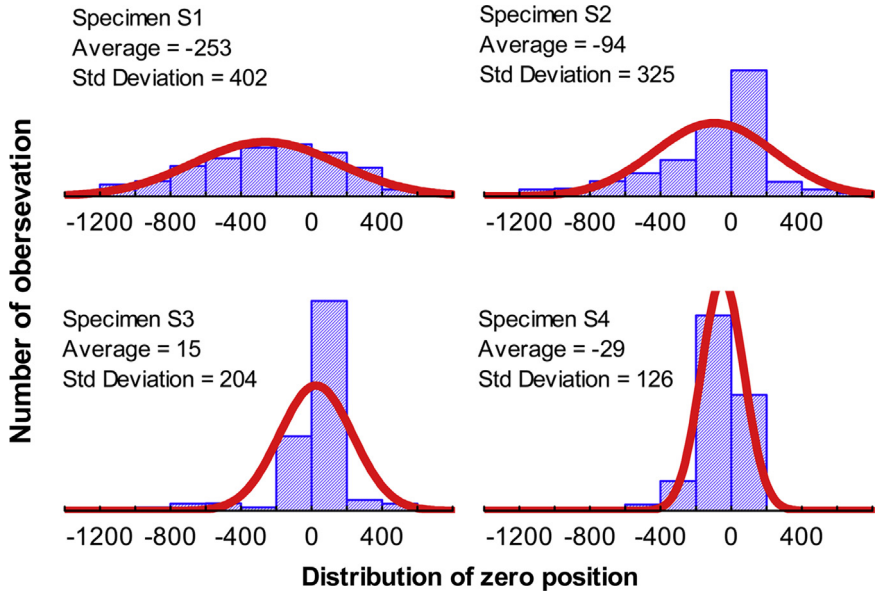

Fig. 5. Distribution of initial contact error for each sandblasted 2017A specimen calculated using a double bootstrap.

4.2. Hardness and ISE factor

In order to observe the effect of initial contact errors on the value of the mechanical properties, the experimental data are treated in two different conditions: ignoring or considering the initial contact errors. These two conditions respectively correspond to the $\Delta h_c = 0$ (not shifting curves) or $\Delta h_c \neq 0$ (shifting curves) in Eq. (9). Fig. 8 shows the value of the macro-hardness H_0 for each sandblasted 2017A specimen calculated with (a) ignoring or (b) considering the initial contact error. First of all, the macro-hardness for the four specimens calculated in condition (a) is in the range of 1.01–1.54 GPa with the standard deviation around 0.1 GPa. For condition (b), the macro-hardness is in the range of 1.63–1.93 GPa with a smaller standard deviation around 0.02 GPa, which is less than the first condition. It is also more accurate than the average value given by the nanoindentation system (around 2 ± 0.3 GPa). Secondly, the mean value of macro-hardness for condition (b) decreases with a decreasing surface roughness from S1 to S4. A possible explanation for this trend is the existence of the strain hardening layer induced by the sandblasting process. In the sandblasting process, a shorter distance for S1 or a stronger jet pressure for S2 means a higher impact stress. This higher impact stress produces a rougher surface and creates a thicker strain hardening layer in the subsurface region, which could change the surface mechanical properties. Thus, the macro-hardness decreases from specimen S1 to S3. The difference of the sandblasting parameters for S3 and S4 is the angle between the jet and the surface. For the smaller angle of S4, the sand particles shoot from a non-vertical direction. This procedure can be divided into two steps: abrading on the initial surface and rebounding from the sandblasted surface [17]. The latter process must dissipate a part of energy done by the sand particles impact. Thus, the work to abrading the initial surface for S4 that the sand particles shooting to the surface with a angle must be weaker than the situation for S1 that sand particles shooting in a vertical direction.

Therefore, the strain hardening layer in S4 is thinner than S3, which denotes a smaller elastic recovery in nanoindentation tests, hence a lower macro-hardness. Moreover, the mean value of macro-hardness given by condition (b) is around 1.5 times the value given by condition (a) for the specimens S1–S3. But this difference is not distinct for specimen S4. Moreover, Fig. 9 shows the ISE factor of each sandblasted 2017A specimen calculated with (a) ignoring or (b) considering the initial contact error.

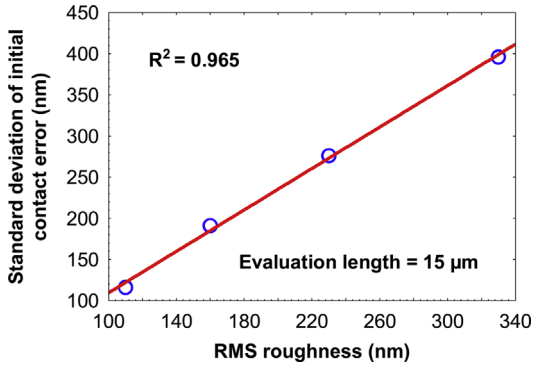

Fig. 7. Linear relation between the standard deviation of initial contact error and the Root Mean Square roughness for the evaluation length equal to 15 μm.

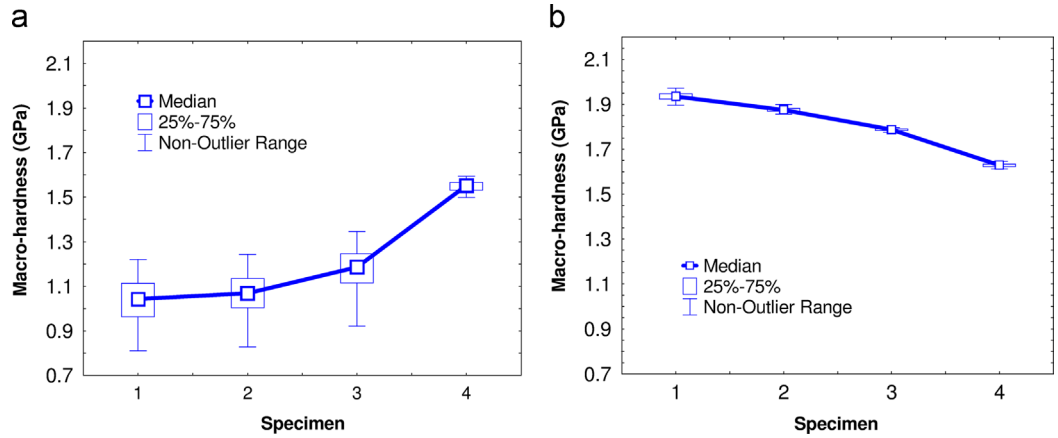

Fig. 8. Macro-hardness for each sandblasted 2017A specimen calculated using novel method (a) ignoring or (b) considering the initial contact error.

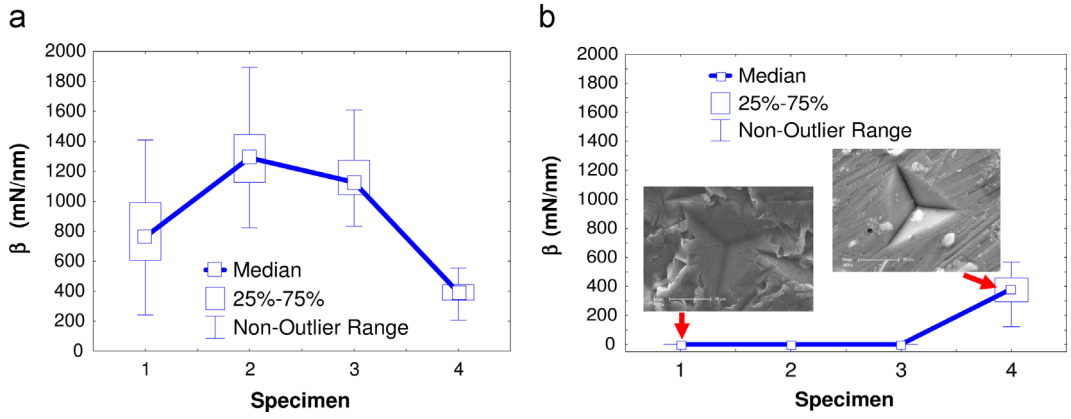

Fig. 9. Indentation size effect factor β for each sandblasted 2017A specimen calculated using novel method (a) ignoring or (b) considering the initial contact error, where the inset figures show an indentation print of specimen S1 (left) and of specimen S4 (right) measured using scanning electron microscopy. The pile-up is the critical origin of ISE for S4.

After considering the initial contact error, the ISE factor becomes zero for the specimens S1–S3. But this factor is almost same for the specimen S4 (around 400 mN/nm). It means except the systemic errors, the initial contact error is directly related with the surface roughness for the specimens having rough surface (S1–S3). This "artificial" ISE can be reduced by considering the initial contact error. For the fine surface S4, the surface roughness is no longer the most important effect on initial contact error. The pile-up around the indentation print is probably the best explanation for the ISE occurrence (inset figures in Fig. 9) [18–20]. This effect will not be diminished by considering the initial contact error. The observation of Fig. 6 permits to note that the difference of the mechanical properties between two conditions decreases with the decreasing of the standard deviation of the initial contact error, which directly relies on the surface roughness (decreases from S1 to S4). It is worth to highlight that the averages of all the initial contact errors are statistically zero even they are a little different with real zero. If infinite indentation curves are studied, the averages of the initial contact errors could equal to zero.

To explain this difference of the value of mechanical properties computed with these two conditions, the loading curves have been simulated by the method described in Section 3.3. For each specimen, one hundred curves are simulated with each standard deviation σ_Δ (variable between 0 and 500 nm) of the distance between the simulated curves and the origin point. The average of the distances between the simulated curves and the origin point is supposed to equal zero, *i.e.* the systemic origin of all the numerical curves is supposed at the zero of the *x*-axis. This distance just corresponds to the initial contact error of the experimental curves. Comparing with the experimental results controlled by all the parameters, the simulated results are just controlled by the imposed standard deviation. Fig. 10 shows the variation of simulated macro-hardness for the four specimens, as a function of the standard deviation of the distance between the origin and the actual position of simulated curves. For each specimen, the average of simulated macro-hardness decreases with the increasing of the imposed standard deviation and it arrives to the highest value when $\sigma_\Delta = 0$. It means the macro-hardness will increase by considering the initial contact error in condition (b). If the standard deviation of initial contact error is lower, the difference of macro-hardness is smaller. It proves the rationality that the difference of macro-hardness between two conditions is bigger for rough surface S1–S3, but smaller for S4. The simulated curves shown in inset figure with different standard deviations (0 nm and 125 nm) can explain this phenomenon. Higher standard deviation corresponds to a bigger dispersion of the simulated curves around zero point. The simulated curves with bigger dispersion just like to flatten the loading curve obtained by applying the proposed model. This flattening process, due to the minimization of the sum of squared residuals of the standard deviation, decreases the macro-hardness of the identified curves.

Table 2 summarizes the mean value and associated standard deviations of macro-hardness for experimental and simulated curves (a) with or (b) without the consideration of initial contact error. The results calculated for experimental and simulated curves in condition (a) are similar. The slight difference is brought principally by the hypotheses in the curve simulation. In the curves simulation, the systemic origin is supposed to be zero.

Table 2
Mean values and associated standard deviation of the macro-hardness of four 2017A specimens.

Specimen	Experimental curves					Simulated curves condition (a): $\Delta h_c = 0$	
	Condition (a): $\Delta h_c = 0$		Condition (b): $\Delta h_c \neq 0$				
	H_0 (GPa)	$\sigma(H_0)$ (GPa)	H_0 (GPa)	$\sigma(H_0)$ (GPa)	$\sigma(\Delta h_c)$ (nm)	H_0 (GPa)	$\sigma(H_0)$ (GPa)
S1	1.01	0.11	1.93	0.0200	402	0.84	0.13
S2	1.06	0.11	1.88	0.0170	325	1.18	0.10
S3	1.17	0.10	1.82	0.0067	204	1.48	0.06
S4	1.54	0.02	1.63	0.0069	126	1.53	0.02

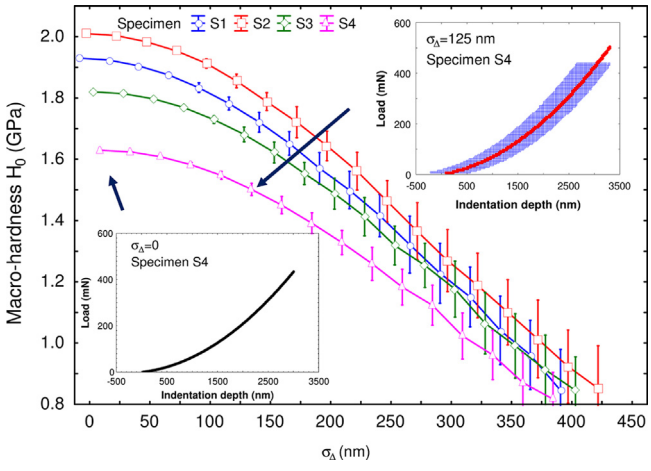

Fig. 10. Variation of the macro-hardness of the simulated curves for the four specimens, as a function of the standard deviation of the distance between the zero and the actual position of the simulated curves. In the inset figures, the thin curves are the simulated loading curves obtained before the optimization while the bold ones obtained after optimization with the proposed model.

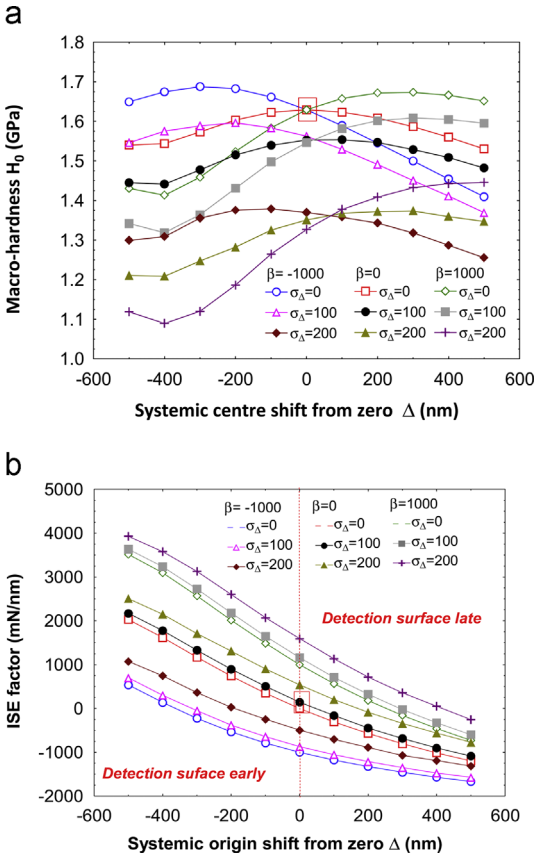

Fig. 11. Variation of the (a) macro-hardness H_0 and (b) ISE factor β for specimen S4. These values were identified using the simulated curves and are represented as a function of the systemic shift from the origin point Δ, for three standard deviations of shifts σ and three ISE factors β.

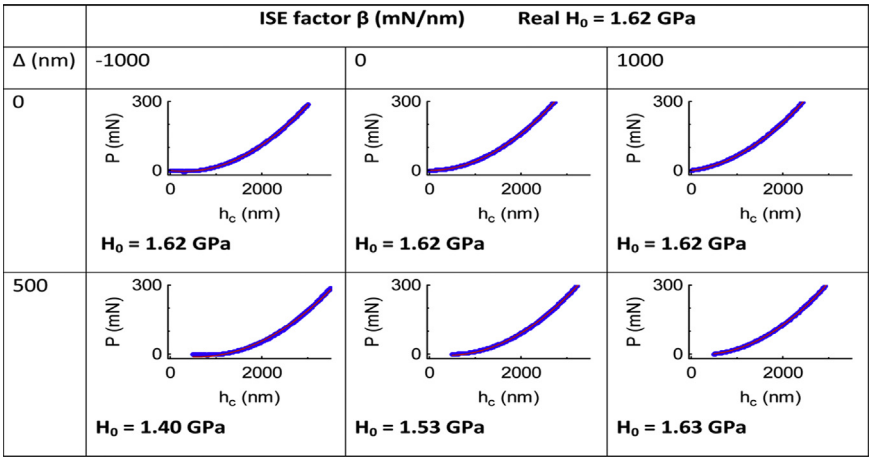

Fig. 12. Simulated curves after the optimization using the proposed model equation (5) with considering or neglecting the initial contact error for specimen S4. In the treatment, the systemic origin shift is equal to 0 nm or 500 nm and the ISE factor is equal to −1000, 0 or 1000 mN/nm. The curve obtained considering the initial contact error is shown in bold while the thin curve is obtained assuming this error is equal to zero.

But this hypothesis strongly relates with the sensibility for the detection of the contact between indenter and surface. It is possible that the systemic origin is not in zero. Therefore, a new simulation with a variable systemic origin of all the numerical curves has been performed. The variable interval of systemic origin is from −500 nm to 500 nm, note as Δ. It is the gap between the systemic origin and the zero of x-axis. Then the simulated curves are placed with three imposed standard deviations of the distance between the systemic origin and the actual position of the curves σ (0, 100 and 200 nm) and three indentation size effect factors β (positive, negative and zero). Fig. 11 shows the results of these new simulations. It could be observed that the error on the position of systemic origin brings the error on the macro-hardness determination. At the same time, the macro-hardness error also depends on the ISE factor and the imposed standard deviation. Fig. 12 represents the simulated curves after the optimization using the proposed model Eq. (9) with considering or neglecting the initial contact error for specimen S4. In the treatment, the systemic origin shift is equal to 0 nm or 500 nm and the ISE factor is equal to −1000, 0 or 1000 mN/nm. The curve obtained considering the initial contact error is shown in bold while the thin curve is obtained assuming this error is equal to zero. But the estimated macro-hardness by later optimization ($\Delta h_c = 0$) are variable when the imposed systemic origin shift and the ISE factor are changed. It clearly means that the negligence of the initial contact error in treatment can induce a bad estimation of the macro-hardness value, even if the curves are similar enough. Some detailed arguments have been given in previous work [21].

5. Conclusions

The proposed initial contact error correction method is able to accurately evaluate the mechanical properties of different aluminum-based alloy 2017A sandblasted samples using nanoindentation test. The estimated macro-hardness is in the range of 1.63–1.93 GPa with a small deviation around 0.02 GPa, which is more accurate than the one calculated by the nanoindentation system using average curves (around 2 ± 0.3 GPa). Furthermore, a multi-scale surface analysis is performed to determine the best evaluation length, which leads to an appropriate description of the surface topography. A linear relation between the standard deviation of the initial contact error and the standard deviation of the amplitude of surface topography is found which clearly highlights the effect of surface roughness on the indentation results. Finally, the best evaluation length for roughness analysis is found to be equal to 15 μm, which is almost of the same order of magnitude as the indentation imprint.

Acknowledgment

Contract grant sponsor: China Scholarship Council (CSC), No. 2010008045.

References

[1] Oliver WC, Pharr GM. Measurement of hardness and elastic modulus by instrumented indentation: advances in understanding and refinements to methodology. J Mater Res 2004;19:3–20.
[2] Fischer-Cripps AC. Critical review of analysis and interpretation of nanoindentation test data. Surf Coat Technol 2006;200:4153–65.
[3] Fischer-Cripps AC. A review of analysis methods for sub-micron indentation testing. Vacuum 2000;58:569–85.
[4] Ullner C. Requirement of a robust method for the precise determination of the contact point in the depth sensing hardness test. Measurement 2000;27:43–51.
[5] Pharr G. Measurement of mechanical properties by ultra-low load indentation. Mater Sci Eng A 1998;253:151–9.
[6] Kalidindi SR, Pathak S. Determination of the effective zero-point and the extraction of spherical nanoindentation stress–strain curves. Acta Mater 2008;56:3523–32.
[7] Brammer P, Bartier O, Hernot X, Mauvoisin G, Sablin SS. An alternative to the determination of the effective zero point in instrumented indentation: use of the slope of the indentation curve at indentation load values. Mater Des 2012;40:356–63.
[8] Bigerelle M, Mazeran PE, Rachik M. The first indenter-sample contact and the indentation size effect in nano-hardness measurement. Mater Sci Eng C 2007;27:1448–51.
[9] Marteau J, Mazeran PE, Bouvier S, Bigerelle M. Zero-point correction method for nanoindentation tests to accurately quantify hardness and indentation size effect. Strain 2012;48:491–7.
[10] Marteau J, Bigerelle M, Xia Y, Mazeran PE, Bouvier S. Quantification of first contact detection errors on hardness and indentation size effect measurements. Tribol Int 2013;59:154–62.
[11] Xia Y, Bigerelle M, Marteau J, Mazeran PE, Bouvier S, Iost A. Effect of surface roughness in the determination of the mechanical properties of material using nanoindentation test. Scanning 2014;36:134–49.
[12] Bigerelle M, Mathia T, Bouvier S. The multi-scale roughness analyses and modeling of abrasion with the grit size effect on ground surfaces. Wear 2012;286:124–35.
[13] Bigerelle M, Van Gorp A, Iost A. Multiscale roughness analysis in injection-molding process. Polym Eng Sci 2008;48:1725–36.
[14] Vingsbo O, Hogmark S, Jçönsson B, Ingemarsson A. Indentation hardness of surface-coated materials. Philadelphia, USA: ASTM STP; 1986.
[15] Bernhardt E. On microhardness of solids at the limit of Kick's similarity law. Z Met 1941;33:135–44.
[16] Bigerelle M, Anselme K. Bootstrap analysis of the relation between initial adhesive events and long-term cellular functions of human osteoblasts cultured on biocompatible metallic substrates. Acta Biomater 2005;1:499–510.

[17] Carter G, Bevan IJ, Katardjiev IV, Nobes MJ. The erosion of copper by reflected sandblasting grains. Mater Sci Eng A 1991;132:231–6.
[18] Iost A, Bigot R. Indentation size effect: reality or artefact? J Mater Sci 1996;31:3573–7.
[19] Lee Y, Hahn J, Nahm S, Jang J, Kwon D. Investigations on indentation size effects using a pile-up corrected hardness. J Phys D Appl Phys 2008;41:074027.
[20] Kim J, Kang S, Lee J, Jang J, Lee Y, Kwon D. Influence of surface-roughness on indentation size effect. Acta Mater 2007;55:3555–62.
[21] Ho HS, Xia Y, Marteau J, Bigerelle M. Influence de l'amplitude de la rugosité de surfaces sablées sur la mesure de dureté par nanoindentation. Matér Technol 2013;101:305–14.